Germline Selection by Meiosis Defends the Transmission of defective Mitochondria with mtDNA variants

Hongying Sha,[1,2*#] Yimin Yang[1*], Sanbao Shi,[1*] Dongmei Ji,[1,2] Jianxin Pan,[1]

1. State Key Laboratory of Medical Neurobiology, Institutes of Brain Science, Reproductive Center, Zhongshan Hospital, Shanghai Medical College, Fudan University, Shanghai 200032, China

2. Center for Reproductive Medicine, Department of Obstetrics and Gynecology, the First Hospital Affiliated for Anhui Medical University, Hefei 230022, China.

* Co-first author

Corresponding author. Email: shahongying@fudan.edu.cn

SUMMARY

Germline selection of mtDNA is vital in maternal inheritance of mtDNA, as it can eliminate severe mtDNA mutations. However, current evidence concerning germline selection at meiosis level comes from incomplete mtDNA sequencing in human first polar body (PB1), which lacks persuasion. Here, we found various variants, including pathogenic mutation sites, present on whole genome of mtDNA in human PB1 compared with its oocyte. And that PB1 mitochondria with mtDNA variants were defective. Afterwards, to further explore how mitochondria enter PB, the defective mitochondria transfer in mouse germline, including cumulus-oocyte-complexes at germinal vesicle and matured oocytes stage. It confirmed that in the first and second meiosis, active purification selected defective mitochondria into PB1 and PB2. Thus, twice meiosis is the last defense system for purifying selection of mtDNA mutations during oogenesis,

which also demonstrated that PB1 and PB2 would be final destination of deleterious mtDNA mutations in germline selection.

INTRODUCTION

Mitochondria and mitochondrial DNA (mtDNA) are inherited exclusively through the maternal lineage of mammals (Babayev et al., 2015). Thus an oocyte containing mutant mtDNA is likely to give birth to affected offspring (Brown et al., 2006). According to statistics, the incidence of mtDNA disease is high, at least 1 in 5000 (Schaefer et al., 2004, 2008). Although mitochondrial DNA has numerous mutation sites, the mtDNA mutation-related diseases we found come from mutations at that few sites. In other words, only a few mtDNA mutations account for the majority of mtDNA disease. This situation suggests that the severe mutations can be selectively eliminated in the female germ line (Lieber et al., 2019, Wei et al., 2019, Fan et al., 2008, Stewart et al., 2008, Shoubridge et al., 2008). The germline selection may contain four levels: genome level (mitochondrial genetic bottleneck), organelle level (autophagocytosis), cellular level (apoptosis in preovulatory follicles) (Stewart et al., 2008, Fan et al., 2008), and meiosis level (Fanti et al., 2017, Gianoarli et al., 2014).

However, in the study to date, selection by meiosis still lacks direct experimental support. Existing evidence support for germline selection by meiosis only comes from incomplete sequencing of mtDNA genome in human first polar body (PB1) (De Fanti et al., 2017, Gianoarli et al., 2014). Moreover, since mtDNA itself is polymorphic, the variants cannot be convincing evidence of mtDNA selection. Furthermore, sequencing is not the most intuitive evidence for meiosis selection of mtDNA variants. As we know, meiosis is a visual and

traceable biological event under a microscope. In light of these characteristics, we can observe mtDNA mutations selected during meiosis by labeling mitochondria, such as live cell fluorescent probes, under a microscope.

In the present study, to address these issues, we compared variants of the entire mtDNA genome in PB1 and its oocytes. Then, the events of mtDNA selection by meiosis were tracked via defective mitochondrial transfer in mouse germline. Our study provides intuitive evidence to support the existence of meiosis selection against mtDNA variants.

RESULTS

Accumulation of mtDNA variants present in human PB1 relative to its oocyte

The donors were twelve women with ages ranging from 25 to 31, named W_1~W_{12}. A total of 18 matured oocytes were obtained from 25 metaphase I oocytes according the rotuine procedure in our lab (Zou et al. 2019). Correspondingly, oocytes denoted by these women were also named in the order of O_1 to O_{12}. Among them, W_1 to W_6 donated one oocyte, respectively. Oocytes denoted by W_1~W_6 were used as mtDNA sequencing of single cell, including single PB1 and oocyte. Whole Genome Amplification (WGA) was applied for amplifying a single PB1 and oocyte genome (Figure.1A). Meanwhile, in order to verify whether WGA alters the genome sequence, two mixed samples (12 polar bodies and 12 oocytes donated by W_7~W_{12} women) were directly lysed to obtain genomes without WGA. Human mitochondrial genomes of all samples were then amplified in 9, 16 or 23 overlapping PCR fragments (Table.S1, Figure.1B). Subsequently, Sanger sequencing was manipulated on a total of 14 mitochondrial

genomes. The sequencing coverage of all single samples and mixed samples (97.39% ~ 99.92%). Percentage mapped to the whole mtDNA genome was significantly higher than other reported studies, which had sequencing coverage of 9-95% and 69.7%, respectively (Fanti et al., 2017, Gianoarli et al., 2014). The ranges of total variants were 9 to 51 (Fig.1C). Various variants present through the whole mtDNA genomes in PB1 compared to its oocytes (Fig.1C, Table.S2, Spreadsheat S1).

Interestingly, in two PB1s from O2 and O6, we found six and one pathogenic mutation sites respectively associated with Cervical Cancer, HPV infection risk (Zhai et al., 2011), Glaucoma (Jeoung et al., 2014, Collins et al., 2016), atherosclerosis (Sazonova et al., 2015, 2017), myocardial infarction (Sazonova et al., 2018), diabetes (Wang et al., 2001, Chinnery et al., 2005, Park et al., 2008), primary open-angle glaucoma (Collins et al., 2016), Prostate Cancer (Petros, et al., 2005, Brandon, et al., 2006), Major Depressive Disorder (Saxena et al., 2006, Rollins et al.,2009), Cardiomyopathy (Khogali et al., 2001, Liu et al., 2013), coronary artery disease (Mueller et al., 2011), Metabolic Syndrome (Saxena et al., 2006, Palmieri et al., 2011), cancer (Brandon, et al., 2006, Liu et al., 2003), Coronary Atherosclerosis (Sawabe et al., 2011) (Fig.1D). These pathogenic mutation sites strongly suggested that mtDNA mutations would be accumulated within PB1. Thus, we then compared the mitochondrial characteristics of human PB1 and its sister oocyte.

Human PB1 Contained defective Mitochondria than its Sister Oocyte

It has been demonstrated that TMRE and $DiIC_1$ (5) accumulate in active mitochondria due to their relative negative charge. As a result, inactive

mitochondria have decreased membrane potential and fail to sequester TMRE and $DilC_1$ (5) (Chazotte 2011). And Rhod2 and Fluo-3 are the most commonly used fluorescent stains to detect inactive mitochondria reflected by intracellular calcium concentration (Orrenius 2015). Thus, TMRE and $DiIC_1$ (5), Rhod2 and Fluo-3 mitochondrial membrane potential assay kit were used to study the mitochondria activation in human PB1s and its oocyte. In experiments, we found that TMRE and $DilC_1$ 5 were absent in human PB1 while TMRE and $DilC_15$ were abundant in human oocyte.(Figure.2A). The fluorescence intensity for TMRE and DilC15 in human PB1 was significantly lower than that of their sister oocytes (Figure.2B, $P<0.05$ ($DilC_15$ $p=0.001$, TMRE $p=0.0263$)). However, high levels of Rhod2 and Fluo-3 accumulated in human PB1 while very low level of signals were found in human oocyte (Figure.2A). The fluorescence intensity for Rhod2 and Fluo-3 in human PB1 was significantly higher than that of their sister oocytes (Figure.2B, $P<0.05$ (Rhod2 $p=0.0237$, Fluo-3: $p=0.0117$)).

These mitochondrial differences between PB1 and its sister oocyte suggested that defective mitochondria with mtDNA mutations was enriched in PB1 compared to its sister oocyte. How was these defective mitochondria with mtDNA mutations enriched in PB1? Could defective mitochondria also be enriched in PB2? To reveal these, we conducted the defective mitochondria transfer in mouse germline, including cumulus-oocyte-complexes at germinal vesicle and oocytes after meiosis I.

The Defective Mitochondria Transfer in GV COCs Revealed Meiosis I actively Selected Defective Mitochondria into PB1

We first monitored the properties of mitochondria in mouse PB1s and its oocytes using TMRE and DiIC1 (5), Rhod2 and Fluo-3 mitochondrial membrane potential assay kit. We found that, like human PB1, mitochondria were defective in mouse PB1s (Figure 2C). The fluorescence intensity for TMRE and DilC15 in mouse PB1 was significantly lower than that of their sister oocytes (Figure.2D, $P<0.0001$). The fluorescence intensity for Rhod2 and Fluo-3 in mouse PB1 was significantly higher than that of their its sister oocytes (Figure.2D, $P<0.0001$). Then we transferred defective mitochondria from PB1 into cumulus-oocyte-complexes at germinal vesicle (GVCOCs) or broken GVCOCs to observe the destination of defective mitochondria during the first meiotic maturation (Figure 3A, B, Movie.S1). We presumed the transferred mitochondria would have three destinations: completely retained in the matured oocyte, completely extruded into PB1 of the matured oocyte, or some mitochondria retained in the oocyte and some into PB1. (Figure.3A). After manipulating and maturing in vitro for 10 hours, 23 oocytes with PB1s were obtained from 60 GVCOCs. We found that 60.87% (14/23) oocytes completely extruded the transferred mitochondria into their PB1s, while the remaining nine oocytes retained the implanted mitochondria in the cytoplasm (Figure.3B, C, Table.S3). For broken GVCOCs group, 15 oocytes with PB1s were obtained from 25 broken GVCOCs after defective mitochondria manipulating and maturing in vitro for 6 hour. However, none of the 15 oocytes extruded the transferred mitochondria into their PB1s. Instead, all transferred mitochondria were retained in the oocytes (Table.S3).

The Defective Mitochondria Transfer in Meiosis II Oocyte Suggested Meiosis II Continue to Select Defective Mitochondria into PB2

Unlike PB1, PB2 can survive to the blastocyst stage (Motosugi, 2005), suggesting that mitochondria in PB2 may be consistent with mitochondrial characteristics in the cytoplasm of fertilized egg. Therefore, we did not sequence the mtDNA genome of PB2. And the consistency between the two has also led us to explore whether PB1 is the final destination of defective mtDNA and whether meiosis II will continue to select defective mitochondria to enter PB2.

We first investigated whether the mitochondrial characteristics in PB2 are the same as those in the fertilized eggs of mouse and human. Although TMRE and DilC1 (5) were visible in mouse and human PB2 (Figure.S1A,C), Rhod 2 and Fluo-3 were rarely seen in mouse and human PB2s (Figure.S1A,C). The fluorescence intensity showed that there were slight differences for defective mitochondria between mouse PB2 and its sister egg, human PB2 and its sister egg (Figure.S1B,D. Mouse, Dilc5 $p=0.0003$, TMRE $p=0.0011$, Rhod2 $p=0.0066$, Fluo-3: $p=0.5196$. Human, Dilc5 $p=0.0167$, TMRE $p=0.0362$, Rhod2 $p=0.0264$, Fluo-3: $p=0.0603$). Compared with the differences between PB1 and its oocyte, these slight differences between PB2 and its sister egg indicated that meiosis II may continue to select defective mitochondria into PB2 if meiosis I did not fully select the defective mitochondria into PB1.

Next, in order to detect the behaviour of the meiosis II for germline selection, defective mitochondria along with the nuclei in mouse PB1 was transferred into an enucleated mouse oocyte to form a reconstructed oocyte, in accordance with PB1 transfer (PB1T) (Wang et al., 2014). Donor mitochondria of mouse oocytes were labelled with 250nM MitoTracker Red. Then PB1T was performed between the stained oocytes and unstained oocytes (Figure.4A, B, Movie S2). Normally, the nucleus is surrounded by the most active mitochondria due to the nuclear

dynamics require energy (Detmer 2007). Thus, to further confirm whether the mitochondria from PB1 are active or defective, we first observed the distribution of mitochondria relative to the nucleus in recombinant oocytes. Eighty-nine recombinant oocytes were obtained from PB1T. Three configurations of donor mitochondria (red mitochondria) distribution related to the nucleus were found in these recombinant oocytes, including front, unilateral, and scattered (Figure.4C, Table.S4), which strongly suggests that mitochondria in PB1 would be defective. After in vitro fertilization of the recombinant oocytes, a red mitochondrial distribution was observed between the PB2 and its embryos at 2-cell stage, as adhered sperm could affect observing fertilized egg at 1-cell stage under the microscope. It is posited that these defective mitochondria have three destinations: completely retained in the embryo, completely extruded along with PB2, or partially retained in the embryo and partially released into PB2 (Figure.4A). After in-vitro fertilization, Seventy-seven fertilized eggs and Seventy-two embryos of 2-cell were obtained. Confocal imaging showed that red mitochondria were fully extruded into PB2 in three configurations of PB1T recombinant oocytes (Figure.4D, Table.S3). To rule out the possibility of selecting donor mitochondria and extruding them into foreign organelles, MitoTracker treated ooplast was transferred into oocytes to form a recombinant oocyte. After *in vitro* fertilization, we found that all MitoTracker treated cytoplasm retained in 25 recombinant oocytes (Figure.S2, Table.S3). These results suggest that the meiosis II also has the ability to select defective mitochondria into PB2 if oocyte contained defective mitochondria.

DISCUSSION

There is accumulating evidence to support the occurrence of mtDNA purifying selection during oogenesis (Lieber et al., 2019, Wei et al., 2019, Fan et al., 2008, Stewart et al., 2008, Shoubridge et al., 2008). This process is of great importance in preventing human mitochondrial disease, as the selection can eliminate deleterious mtDNA mutations that escape from genetic bottlenecks, and prevent the offspring from inheriting deleterious mtDNA. Although two studies have provided sequencing evidence in supporting the existence of mtDNA purifying selection during the two meiosis, no intuitive experimental data confirms that meiosis I and II have the function of selecting mutant mtDNA. In addition, the variation of sequencing coverage is too fluctuating among samples owing to the low content of mtDNA in PBs in these studies (De Fanti et al., 2017, Gianoarli et al., 2014). Based on almost 100% mtDNA sequencing coverage, our study demonstrated that mitochondria in PB1 accumulate more mtDNA variants and are defective than mitochondria in their sister oocyte. Furthermore, defective mitochondria transfer in mouse germline showed that both meiosis I and II can extrude defective mitochondria with mutant mtDNA into PB1 and PB2, which strongly enhances the occurrence of mtDNA germline selection at meiosis level.

For the failure to excrete the transplanted mitochondria into PB1 in nine oocytes from GVCOCs group and all oocytes from broken GVCOCs group, we speculated that these GVCOCs were in the advanced GV or MI stage. As we know, cytoplasmic streaming is important for the transport of maternal factors , leading to spindle migration and the establishment of oocyte polarity related to the eventual embryonic anterior–posterior polarity during oogenesis (Duan et al.,2019, Gutzeit et al., 1982, Wolke et al., 2007). We speculated the defective

mitochondria was transported with the streaming and the migration of the spindle to the side where the meiosis I would occur in the future. When the meiosis I happened, defective mitochondria with half of the chromosomes extruded to form PB1. When the transplanted mitochondria entered the ooplast of advanced GV or MI oocytes, they might miss the role of cytoplasmic streaming. Then the transplanted mitochondria could not be transported with the migration of the spindle to the side, resulting in the failure to excrete the transplanted mitochondria into PB1.

Hereditary mitochondrial diseases cause a range of serious diseases that can be potentially fatal[1]. It has been noticed that trace amounts of pathogenic mtDNA are conserved in mitochondria replacement, and subsequently outcompete denoted healthy mtDNA, resulting in a reversal to a pathogenic genotype, also known as mitochondrial reversion (Connor 2017, Greenfield 2017). Recently, we have shown that PB1T has the potential to prevent the transmission of mitochondrial diseases from mothers to children and their offspring, as PB1T resulted in undetectable levels of "mutant" mitochondria in mice (Wang et al., 2014, Koch et al., 2014). In this study, our results further provide strong evidence that PB1T has greater potential to thwart mitochondrial reversion in mitochondria replacement, as mitochondria in PB1 is defective and meiosis II can totally squeeze out the mitochondria into PB2 after PB1T following *in vitro* fertilization. Thus, this study also proves the safety and effectiveness of PB1T as it has the potential to prevent mitochondrial reversion in mitochondria replacement.

REFERENCES

247 Babayev, E., Seli, E. (2015). Oocyte mitochondrial function and reproduction. Curr
248 Opin Obstet Gynecol. *27*, 175-81.
249 Bannwarth, S., Procaccio, V., and Paquis-Flucklinger, V. (2009). Rapid identification
250 of unknown heteroplasmic mitochondrial DNA mutations with mismatch-specific
251 surveyor nuclease. In Mitochondrial DNA. (Humana Press), pp. 301-313.
252 Brandon, M., Baldi, P., and Wallace, D.C. (2006). Mitochondrial mutations in
253 cancer Oncogene. *25*, 4647-4662.
254 Brown, D.T, Herbert, M., Lamb, V.K., Chinnery, P.F., Taylor, R.W., Lightowlers,
255 R.N., Craven, L., Cree L., Gardner, J.L., and Turnbull, D.M. (2006). Transmission of
256 mitochondrial DNA disorders: possibilities for the future. Lancet *368*, 87–89.
257 Chazotte, B. (2011). Labeling mitochondria with TMRM or TMRE. Cold Spring
258 Harb. Protoc. *7*, 895-7.
259 Chinnery, P.F., Elliott, H.R., Patel, S., Lambert, C., Keers, S.M., Durham, S.E.,
260 McCarthy, M.I., Hitman, G.A., Hattersley, A.T., and Walker, M. (2005). Role of the
261 mitochondrial DNA 16184-16193 poly-C tract in type 2 diabetes. Lancet *366*, 1650-
262 1651.
263 Collins, D.W., Gudiseva, H.V., Trachtman, B., Bowman, A.S., Sagaser, A., Sankar, P.,
264 Miller-Ellis, E., Lehman, A., Addis, V., and O'Brien, J.M. (2016). Association of
265 primary open-angle glaucoma with mitochondrial variants and haplogroups common
266 in African Americans. Mol. Vision *22*, 454-471.
267 Connor, S. (2017). When replacement becomes reversion. Nat. Biotechnol. *35*,1012–
268 1015.
269 Detmer, S.A., and Chan, D.C. (2007). Functions and dysfunctions of mitochondrial
270 dynamics. Nat. Rev. Mol. Cell. Bio. *8*, 870-879.
271 De Fanti, S., Vicario, S., Lang, M., Simone, D., Magli, C., Luiselli, D., Gianaroli, L.,

and Romeo, G. (2017). Intra-individual purifying selection on mitochondrial DNA variants during human oogenesis. Hum. Reprod. *32*, 1100–1107.

Fan, W., Waymire, K.G., Narula, N., Li, P., Rocher, C., Coskun, P.E., Vannan M.A., Narula, J., Macgregor, G.R., and Wallace, D. C. (2008). A mouse model of mitochondrial disease reveals germline selection against severe mtDNA mutations. Science *319*, 958-962.

Gianaroli, L., Luiselli, D., Crivello, A.M., Lang, M., Ferraretti, A.P., De Fanti, S., Magli, M.C., and Romeo, G. (2014). Mitogenomes of Polar Bodies and Corresponding Oocytes. PloS one., *9*, e102182.

Greenfield, A., Braude, P., Flinter, F., Lovell-Badge, R., Ogilvie, C., and Perry, A.C.F. (2017) Assisted reproductive technologies to prevent human mitochondrial disease transmission. Nat. Biotechnol. *35*,1059–1068.

Gutzeit, H. O. and Koppa, R. (1982). Time-lapse film analysis of cytoplasmic streaming during late oogenesis of Drosophila. J. Embryol. Exp. Morphol. *67*, 101–111.

Jeoung, J.W., Seong, M.W., Park, S. S., Kim, D.M., Kim, S.H., and Park, K.H. (2014). Mitochondrial DNA variant discovery in normal-tension glaucoma patients by next-generation sequencing. Invest. Ophthalmol. Visual Sci. *55*, 986-992.

Khogali, S.S., Mayosi, B.M., Beattie, J.M., McKenna, W.J., Watkins, H., and Poulton, J. (2001). A common mitochondrial DNA variant associated with susceptibility to dilated cardiomyopathy in two different populations. Lancet *357*, 1265-1267.

Koch, L. (2014). Mitochondrial replacement techniques under the spotlight. Nat. Rev. Genet. *15*, 516.

Lieber, T., Jeedigunta, S. P., Palozzi, J. M., Lehmann, R., and Hurd, T. R. (2019).

297 Mitochondrial fragmentation drives selective removal of deleterious mtDNA in the
298 germline. Nature *569*, 1-5.
299 Liu, S., Bai, Y., Huang, J., Zhao, H., Zhang, X., Hu, S., and Wei, Y. (2013). Do
300 mitochondria contribute to left ventricular non-compaction cardiomyopathy? New
301 findings from myocardium of patients with left ventricular non-compaction
302 cardiomyopathy. Mol. Genet. Metab. *109*, 100-106.
303 Liu, V.W., Wang, Y., Yang, H.J., Tsang, P.C., Ng, T.Y., Wong, L.C., Nagley, P., and
304 Ngan, H.Y. (2003). Mitochondrial DNA variant 16189T>C is associated with
305 susceptibility to endometrial cancer. Hum. Mut. *22*, 173-174.
306 Motosugi, N., Bauer, T., Polanski, Z., Solter, D., and Hiiragi, T. (2005). Polarity of the
307 mouse embryo is established at blastocyst and is not prepatterned. Genes Dev. *19*,
308 1081-1092.
309 Mueller, E. E., Eder, W., Ebner, S., Schwaiger, E., Santic, D., Kreindl, T., Stanger, O.,
310 Paulweber, B., Iglseder, B., Oberkofler, H., et al. (2011). The mitochondrial
311 T16189C polymorphism is associated with coronary artery disease in Middle
312 European populations. PLoS One. *6*, e16455.
313 Orrenius, S., Gogvadze, V., and Zhivotovsky, B. (2015). Calcium and mitochondria in
314 the regulation of cell death. Biochem. Bioph. Res. Co. *460*, 72-81.
315 Palmieri, V.O., De Rasmo, D., Signorile, A., Sardanelli, A.M., Grattagliano, I.,
316 Minerva, F., Cardinale, G., Portincasa, P., Papa, S., and Palasciano, G. (2011).
317 T16189C mitochondrial DNA variant is associated with metabolic syndrome in
318 Caucasian subjects. Nutrition. *27*, 773-777.
319 Park, K.S., Chan, J.C., Chuang, L.M., Suzuki, S., Araki, E., Nanjo, K., Ji, L., Ng, M.,
320 Nishi, M., Furuta, H., et al. (2008). A mitochondrial DNA variant at position 16189 is
321 associated with type 2 diabetes mellitus in Asians. Diabetologia. *51*, 602-608.

Petros, J.A., Baumann, A.K., Ruiz-Pesini, E., Amin, M.B., Sun, C.Q., Hall, J., Lim, S., Issa, M.M., Flanders, W. D., Hosseini, S. H., et al. (2005). mtDNA mutations increase tumorigenicity in prostate cancer. Proc. Natl. Acad. Sci. USA. *102*, 719-724.

Rollins, B., Martin, M.V., Sequeira, P.A., Moon, E.A., Morgan, L.Z., Watson, S.J., Schatzberg, A., Akil, H., Myers, R.M., Jones, E.G., et al. (2009). Mitochondrial variants in schizophrenia, bipolar disorder, and major depressive disorder. PLoS One *4*, e4913.

Sawabe, M., Tanaka, M., Chida, K., Arai, T., Nishigaki, Y., Fuku, N., Mieno, M.N., Kuchiba, A., and Tanaka, N. (2011). Mitochondrial haplogroups A and M7a confer a genetic risk for coronary atherosclerosis in the Japanese elderly: an autopsy study of 1,536 patients. J. Atheroscler. Thromb. *18*, 166-175.

Saxena, R., de Bakker, P.I., Singer, K., Mootha, V., Burtt, N., Hirschhorn, J.N., Gaudet, D., Isomaa, B., Daly, M.J., Groop, L., et al. (2006). Comprehensive association testing of common mitochondrial DNA variation in metabolic disease. Am. J. Hum. Genet. *79*, 54-61.

Sazonova, M.A., Ryzhkova, A.I., Sinyov, V.V., Galitsyna, E.V., Melnichenko, A.A., Demakova, N.A., Sobenin, I.A., Shkurat, T.P., and Orekhov, A.N. (2018). Mitochondrial genome mutations associated with myocardial infarction. Disease Markers. *2018*, 1-6.

Sazonova, M.A., Sinyov, V.V., Barinova, V.A., Ryzhkova, A.I., Zhelankin, A.V., Postnov, A.Y., Sobenin, I.A., Bobryshev, Y.V., and Orekhov, A.N. (2015). Mosaicism of mitochondrial genetic variation in atherosclerotic lesions of the human aorta. BioMed Res. Int. *2015*, 1-9.

346 Sazonova, M.A., Sinyov, V.V., Ryzhkova, A.I., Galitsyna, E.V., Khasanova, Z.B.,
347 Postnov, A.Y., Yarygina, E.I., Orekhov, A.N., and Sobenin, I.A. (2017). Role of
348 mitochondrial genome mutations in pathogenesis of carotid atherosclerosis. Oxid.
349 Med. Cell. Longevity. *2017*, 1-7.
350 Schaefer, A.M., McFarland, R., Blakely, E.L., He, L., Whittaker, R.G., Taylor, R.W.,
351 Chinnery P.F., and Turnbull, D.M. (2008). Prevalence of mitochondrial DNA disease
352 in adults. Ann. Neurol. *63*, 35-39.
353 Schaefer, A.M., Taylor, R.W., Turnbull, D.M., and Chinnery, P.F. (2004). The
354 epidemiology of mitochondrial disorders—past, present and future. Biochim.
355 Biophys. Acta, Bioenerg. *1659*, 115-120.
356 Shoubridge, E.A., and Wai, T. (2008). Sidestepping mutational
357 meltdown. Science, *319*, 914-915.
358 Stewart, J. B., Freyer, C., Elson, J. L., and Larsson, N. G. (2008). Purifying selection
359 of mtDNA and its implications for understanding evolution and mitochondrial
360 disease. Nat. Rev. Genet. *9*, 657.
361 Wang, D., Taniyama, M., Suzuki, Y., Katagiri, T., and Ban, Y. (2001) Association of
362 the mitochondrial DNA 5178A/C polymorphism with maternal inheritance and onset
363 of type 2 diabetes in Japanese patients. Exp. Clin. Endocrinol. Diabetes *109*, 361-
364 364.
365 Wang, T., Sha, H., Ji, D., Zhang, H.L., Chen, D., Cao, Y., and Zhu, J. (2014). Polar
366 body genome transfer for preventing the transmission of inherited mitochondrial
367 diseases. Cell *15*, 1591-1604.
368 Wei W., Tuna S., Keogh MJ., Smith K.R., Aitman T.J., Beales P.L., Bennett D.L., Gale
369 D.P., Bitner-Glindzicz M.A.K., Black G.C., et al. (2019). Germline selection shapes
370 human mitochondrial DNA diversity. Science *364*, eaau6520.

371 Wolke, U., Jezuit, E. A. and Priess, J. R. (2007). Actin-dependent cytoplasmic
372 streaming in C. elegans oogenesis. Development *134*, 2227–2236.
373 Zhai, K., Chang, L., Zhang, Q., Liu, B., and Wu, Y. (2011). Mitochondrial C150T
374 polymorphism increases the risk of cervical cancer and HPV infection.
375 Mitochondrion. *11*, 559-563.
376 Zou et al. lMelatonin promotes the development of immature oocytes from the
377 COH cycle into healthy offspring by protecting mitochondrial function. J Pineal
378 Res. 2020; 68: e12621. https://doi.org/10.1111/jpi.12621.
379

380 **AUTHOR CONTRIBUTIONS**

381 H.S. supervised and designed the experiments. H.S. and D.J manipulated
382 mitochondrial transfer. J.Pan. manipulated mtDNA sequence. Y.Yang., S.S and
383 J.Pan. performed staining and confocal analysis. S.S supervised mice and
384 collected oocytes. H.S. and Y.Yang. prepared the figures and wrote the
385 manuscript.

386 **ACKNOWLEDGMENT**

387 This study was supported by grants from National Natural Science Foundation of
388 China (National NSF grants 31871506, Basic key projects of Shanghai Science
389 and Technology Commission 19JC1411200 and 81471512 to H.S.). The authors
390 declare no conflict of interests.
391
392
393
394

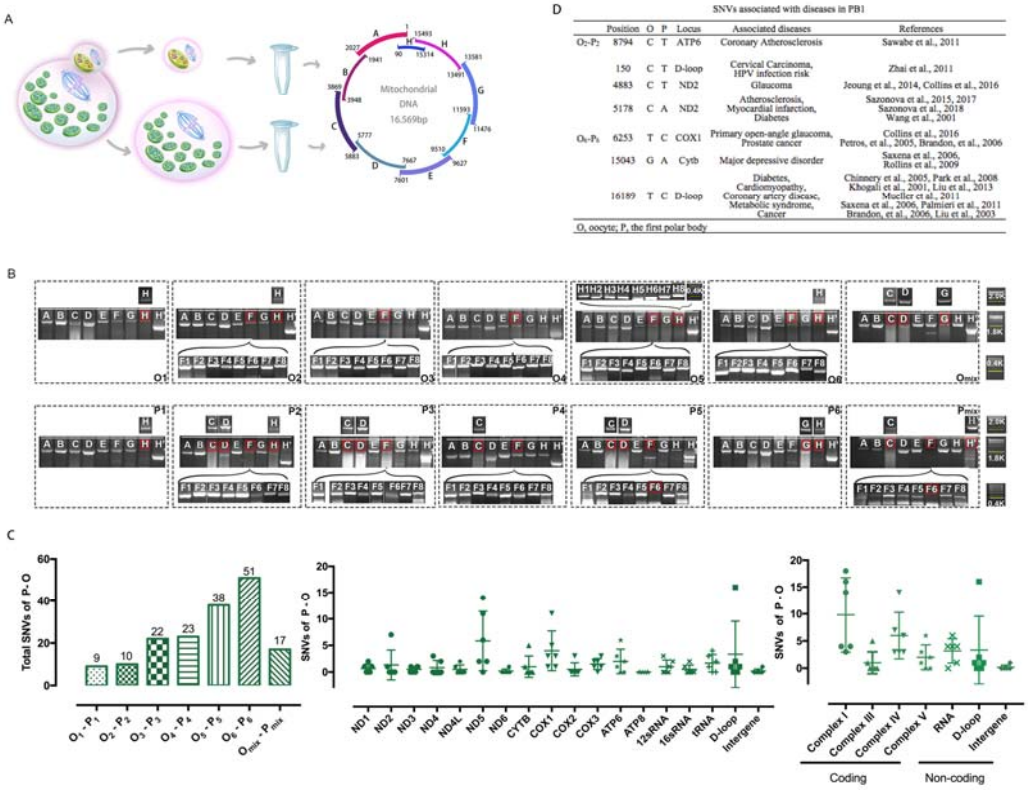

Figure.1. Accumulation of mtDNA variants present in human PB1 relative to its oocyte

A. Schematic charts of experimental design of sequencing mtDNA variants in human PB1 and oocyte. B. Amplicons (A-H') and (F1-F8, H1-H8) of mitogenomes from each single oocyte and PB1. An electrophoresis map represents each amplified fragment of a single oocyte and PB1 sample. Red boxes marked those fragments that failed to be amplified or sequenced. M, size marker. C. Comparison of total mtDNA variants between PB1 and its sister oocyte. Distribution of mtDNA variants in different regions compared to PB1 and its sister oocyte. Total mtDNA variants in coding and non-coding regions compared between PB1 and

its sister oocyte. D. SNVs associated with diseases in mtDNA.

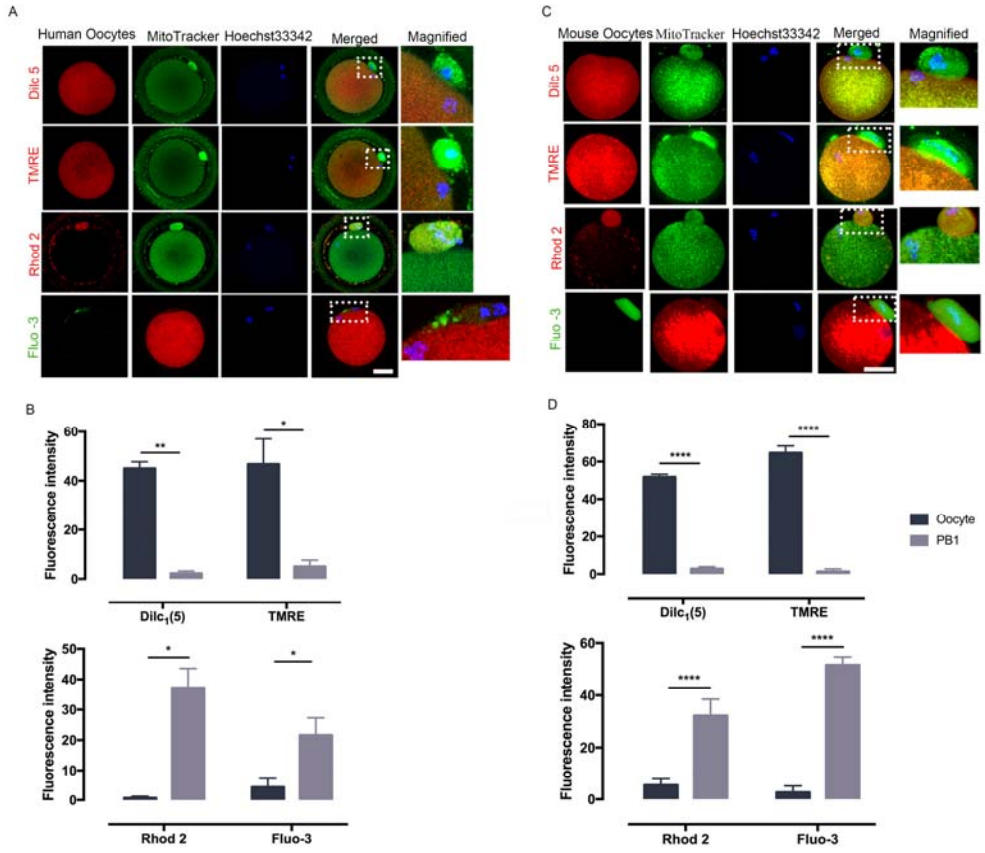

Figure.2. Human and mouse PB1 Contain defective mitochondria than its Sister Oocyte

A. Mitochondrial membrane potential was detected with TMRE and DilC1(5), Rhod2 and Fluo-3 in human PB1 and oocytes. B. The relative fluorescence intensity of human PB1 to its sister oocyte was quantified and the difference significance was evaluated using paired t test. C. Mitochondrial membrane potential was detected with TMRE and DilC1(5), Rhod2 and Fluo-3 in mouse PB1 and oocytes. D. The relative fluorescence intensity of mouse PB1 to its sister oocyte was quantified and the difference significance was evaluated using paired

421 t test. In TMRE and DilC1(5), Rhod2 detection, red color represented TMRE and
422 DilC1(5), Rhod2, green color marked mitochondria in PB1 and oocyte. In Fluo-3
423 detection, green color showed Fluo-3, red color stained mitochondria in PB1 and
424 oocyte. ****p < 0.0001, ***p < 0.001, **p < 0.01, *p < 0.05. Error bars indicate SD,
425 with the mean value. n=3 per group for human, n = 6 per group for mouse. Scale
426 bar=40μm.
427
428

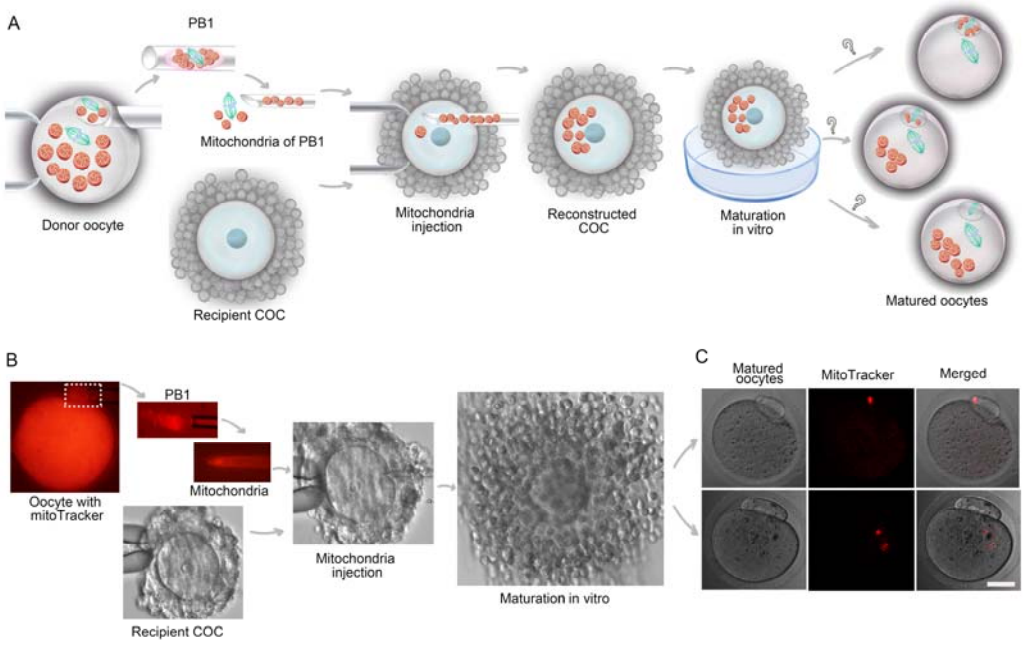

429

430 **Figure.3. Meiosis I Selected defective Mitochondria into PB1**

431 A. Schematic charts of experimental design of defective mitochondria transfer at
432 GVCOCs and broken GVCOCs stage in this study. B. Micromanipulation of
433 defective mitochondria transfer in GVCOCs in this study. Donor oocyte stained
434 with MitoTracker red, then mitochondria (red) in PB1 was isolated and injected
435 into GVCOCs or broken GVCOCs. Subsequently, the COC was matured in vitro for
436 10 or 4~5 hours for the GVCOC or broken GVCOCs, respectively. C. Red

437 mitochondria distribution in the PB1 and its oocyte from the matured COCs.
438 Scale bar=40μm.
439
440

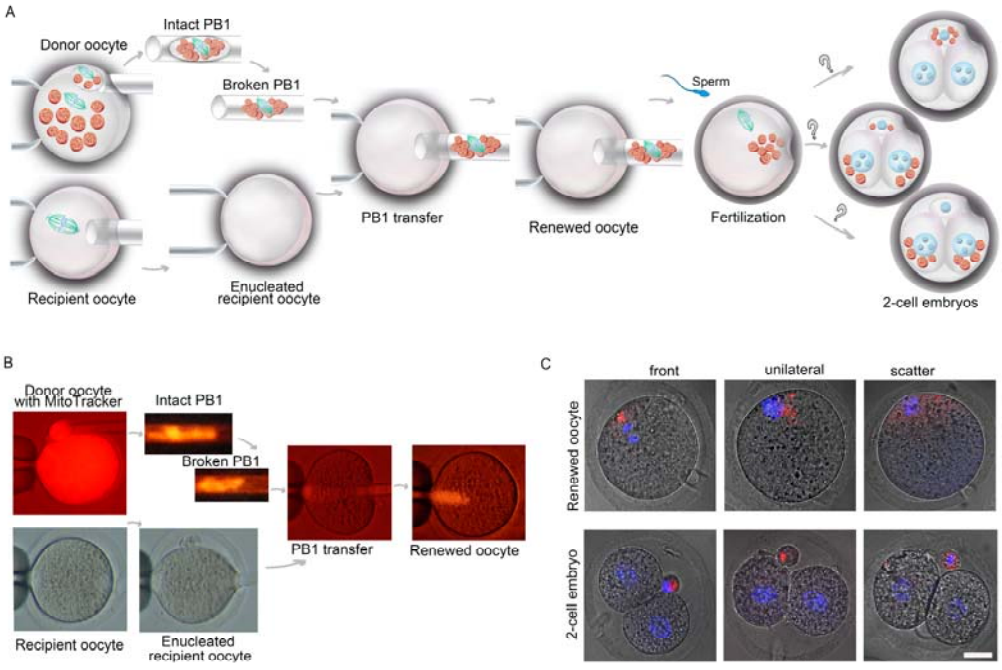

441

442 **Figure.4. Meiosis II Continue to Select defective Mitochondria into PB2**

443 A. Schematic charts of experimental design of mitochondria transfer at prophase
444 of meiosis II in this study. B. Micromanipulation of mitochondria transfer at
445 prophase of meiosis II in this study: Donor oocyte stained with MitoTracker red,
446 PB1 isolation, recipient oocyte and enucleated oocyte, recombinant oocyte with
447 PB1 genome and mitochondria (red). C. top row: Recombinant oocytes from
448 mitochondria transfer, including three configurations of donor mitochondria
449 (red mitochondria) distribution relative to donor nuclei: front, scattered and
450 unilateral type. Next layer : embryos at 2-cell stage from the recombinant
451 oocytes. Red mitochondria in all type of PB1T recombinant oocytes were totally

452 expelled into PB2. Scale bar=40μm.

453

454

455 **MATERIALS AND METHODS**

456 **Human oocytes and egg donations**

457 This study was approved by the Institutional Review Board of the First Affiliated
458 Hospital (research license 20160022, 20140222), Anhui Medical University. All
459 the infertile patients agreed and signed informed consent in advance. Totally, 11
460 patients, who were undergoing regular in-vitro fertilization (IVF) at our
461 reproductive center, donated 25 oocytes for sequencing in this study. Another 15
462 patients donated 12 oocytes and 12 zygotes for MitoTracker probes staining. All
463 human oocytes in this study were (those) immature oocytes from controlled ovarian
464 hyperstimulation (COH). Since these oocytes must be denuded for ICSI, the meiotic
465 status of these denuded oocytes can be investigated on the morphological grading
466 under microscopic evaluation. All retrieved oocytes were categorized as metaphase II
467 (MII) oocytes, metaphase I (MI), and germinal vesicle (GV). All mature metaphase II
468 (MII) oocytes were used for conventional ICSI. Oocytes at MI stage were donated for
469 this study (Zou et al, 2019). Oocytes at MI stage were maturated in vitro for about
470 24 hours and monitored under microscopy to observe PB1 extrusion. As soon as PB1
471 extrusion for about 2 hours, oocyte and its PB1 were isolated for mtDNA sequencing.

472 **Animals**

473 B6D2F1 (C57/BL6×DBA) was used in this study. All mice used in this study
474 were maintained in accordance with the guidelines of the Laboratory Animal
475 Service, Fudan University (research license 20160225-103).

476 **Media for manipulation and culture of oocytes and embryos**

In this study , the media for the manipulation and culturing oocytes and zygotes were from Vitrolife Sweden AB, Goteborg, Sweden.

mtDNA genome sequencing

Zone pellucida of oocytes was digested by 0.5% pronase (Roche, 70229227) in 37°C for 5 min. The single oocyte or polar body was sorted into 4 μl PBS. Then 3 μl buffer D2 was added and incubated at 65 °C for 10 min, followed by adding 3 μl stop solution. The lysised products of oocytes were diluted 1:10 and polar bodies were not. Then each PB1 sample was amplified with whole genome amplification (WGA) using REPLI-g Single Cell Kit (QIAGEN, 150345). For each oocyte sample, one-tenth of lysised product was applied for amplification. The DNA concentration was determined by Infinite 200 PRO NanoQuant (TECAN) and diluted to 150ng/μl. Then mtDNA genome of each sample was amplified in 50 μl reaction volume containing 10 μl 5X GC buffer, 1.5 mM Mg^{2+}, 200 nM dNTP, 1 μM of each primer, 0.2 μl (1 unit) Taq DNA Polymerase and 1μl template using 9 pair primers (A-H') (Table S1) (Bannwarth et al., 2009). The PCR was under the following condition: 95°C for 5 min; 38 cycles with denaturation at 95°C for 20 s, annealing at 57°C for 30 s, and elongation at 72°C for 1 min; 1 cycle at 72°C for 10 min with a final 25°C for 10 s (Bannwarth et al., 2009). After estimated by electrophoregram, the PCR products were sequenced using 3730xl DNA Analyzer (ABI). Electropherograms were inspected and aligned to the revised Cambridge reference sequence (NC_012920) using Sequencher 5.4.5. For those mtDNA regions that failed to be amplified or sequenced, PCR reactions were repeated (Figure S1), or new primers (F1-F8, H1-H8) were designed to amplify the failed regions (Table S1). The PCR with F1-F8 and H1-H8 primers under the following condition: 95°C for 5 min; 38 cycles with denaturation at 95°C for 15 s, annealing at 57°C for 15 s, and elongation at 72°C for

30 s; 1 cycle at 72°C for 7 min with a final 25°C for 10s.

For two mix samples of twelve oocytes and twelve PB1s in this study, their lysised products were directly applied to amplify mtDNA genome without WGA

Sequence Analysis

A Plasmid Editor (APE) software was used to align mtDNA sequences of every two samples. Nucleotides that failed to be sequenced were marked as 'N' in sequences. The Mitomap (www.mitomap.org) was used to identify locus of variants and make the functional annotation of AAs change and associated diseases previously reported.

Membrane potential detection of Mitochondrial

Mouse oocytes were collected at hCG 12.5 to 14 hours. TMRE, DilC 5, Rhod-2 and Fluo Calcium Indicator (Fluo-3 AM) were applied to detect Mitochondrial membrane potential. For TMRE (ab113852, Abcam), $DilC_1(5)$ (M34151, life Technology) and Rhod-2 (M34151, life Technology) staining, MitoTracker (MitoTracker Green FM, M7514, Life Technology) were used to locate the mitochondria. For Fluo-3AM, MitoTracker (MitoTracker Red CMXRos, M7512, Life Technology) was applied to located the mitochondria. Live oocytes were styed at 37°C for 30 minutes and incubated in G-gamete buffer at 37°C for 20mins afterwards. Images were taken with leica confocal scanning microscope.

The defective mitochondria transfer in mouse germline

Mitochondria transfer at Germinal vesicle stage

Donor mouse oocytes with PB1 were retrieved at HCG 12 hours, cumulus -oocyte-cumulus complexes were released from ovarian follicles into G-gamete. Cumulus cells were denuded by 3 minutes at incubation with 0.1% hyaluronidase (Sage IVF). Denuded Oocytes with PB1s were stained with 250nM MitoTracker (MitoTracker Red CMXRos, M7512, Life Technology) for 0.5 hour. The mitochondria in PB1 were

isolated with 10 and 5.5μm noodle.

Recipient cumulus-oocyte-complexes at GV stage (GVCOCs) were retrieved from ovarian follicles into G-gamete at HCG 5 hours. Then one cumulus-oocyte-complex at GV stage (GVCOCs) or broken GV stage was selected and fixed to the holding needle by applying a vacuum, the mitochondria in 5.5μm noodle were transferred into the ooplast of GVCOCs using microinjection manipulation via 3 clock direction. Subsequently, the GVCOCs and broken GVCOCs were matured in vitro for 10 and 5 hours, respectively. Images of matures oocytes were taken with leica confocal scanning microscope. See also supplemental movie 1.

Mitochondria transfer at the second meiosis

Cumulus-oocyte-cumulus complexes were released from both ovarian follicles (donor oocytes) and oviducts (recipient oocytes) into G-gamete. Cumulus cells were denuded by 3 minutes at incubation with 0.1% hyaluronidase (Sage IVF). Denuded Oocytes were cultured in G1 medium at 37.5°C, in 5% CO_2, 5% O_2, and 90% N_2 incubation for 30 min before further treatments. Donor mouse oocytes with PB1 were dyed with 250nM MitoTracker. Then mitochondria transfer was performed between PB1 of stained donor oocytes and unstained recipient oocytes using the first polar body genome transfer (PB1T) (Wang et al., 2014). Then PB1T oocytes were fertilized in vitro. Detailed methods for PB1T and IVF were processed according to the previously described methods (Wang et al., 2014). Images of 2-cell embryos were taken with leica confocal scanning microscope. See also supplemental movie 2.

The active mitochondria transfer (ooplast transfer) in mouse germline

Mouse oocytes at meiosis II were dyed with 250nM MitoTracker. Then ooplast transfer was performed between stained mouse oocytes and unstained mouse

552 oocytes to form reconstructed oocyte. Then reconstructed oocytes were
553 fertilized in vitro. Detailed methods for ooplast transfer and IVF of the
554 reconstructed oocytes were processed according to the previously described
555 methods (Wang et al., 2014). See also supplemental movie 3. Images of 2-cell
556 embryos were taken with leica confocal scanning microscope.

557 **Statistical Analysis**

558 GraphPad Prism 7 was used to conduct the statistical data analysis. Unpaired t test
559 was performed for the relative fluorescence intensity of the relative fluorescence
560 intensity of human and mouse PB1 to their sister oocyte, human and mouse PB2
561 to their sister egg, where the significance was set at $p < 0.05$ (* represents $p < 0.05$,
562 ** represents $p < 0.01$, *** represents $p < 0.001$, **** represents $p < 0.0001$).